Am J Transl Res 2019;11(6):3707-3721
www.ajtr.org /ISSN:1943-8141/AJTR0093317

Original Article

The protective effects of bone mesenchymal stem cells on paraquat-induced acute lung injury via the muc5b and ERK/MAPK signaling pathways

Lichun Zhang, Qiuhe Li, Zhenning Liu, Yu Wang, Min Zhao

Department of Emergency, Shengjing Hospital Affiliated to China Medical University, No. 36 Sanhao Street, Heping District, Shenyang 110004, Liaoning Province, China

Received March 4, 2019; Accepted May 17, 2019; Epub June 15, 2019; Published June 30, 2019

Abstract: Objective: To evaluate the protective effect of bone mesenchymal stem cells (BMSCs) on paraquat (PQ)-induced acute lung injury (ALI) and investigate the possible underlying mechanisms. Methods: Male Sprague Dawley rats were treated with BMSCs (3×10^6) 1 h after intraperitoneal injection of PQ. The cell apoptosis rate and mitochondrial membrane potential in rat pulmonary alveolar type II epithelial (ATII) cells were quantitated by flow cytometry. IL-17, IL-6, and MUC5B levels in bronchoalveolar lavage fluid (BALF) and ATII culture medium were measured. Lung tissues were collected to determine the wet-to-dry (W/D) ratios and lung injury scores, in addition to the protein and mRNA expression levels of ERK1/2, Bcl-2, Bax, and muc5b. Results: BMSCs had decreased mRNA expression of Muc5b in lung tissue of rats with PQ-induced ALI as shown by RNA-seq. Treatment with BMSCs also alleviated the PQ-induced increases in protein expression in the BALF and reduced the concentration of IL-17, IL-6, and Muc5b in both the BALF and ATII culture medium. In addition, the ATII cell apoptosis rate and mitochondrial membrane potential, as well as the W/D ratios, were decreased by BMSC treatment. Moreover, BMSCs ameliorated the expression levels of *Bax* mRNA and active caspase-3 proteins and increased *Bcl-2* mRNA expression. Furthermore, BMSCs attenuated ERK1/2 activation upon PQ-induced ALI in lung tissue. Conclusion: BMSC therapy can protect against PQ-induced ALI in rats. A possible mechanism is the suppression of the muc5b and ERK/MAPK signaling pathways, resulting in an improvement in the endothelial permeability and a decrease in inflammation and cell apoptosis.

Keywords: Bone marrow derived mesenchymal stem cells, paraquat poisoning, acute lung injury, Muc5b and ERK/MAPK signaling pathways

Introduction

Paraquat (1,1-dimethyl-4,4-bipyridilium dichloride, PQ) has an excellent weeding effect but a strong toxicity to humans and animals, and its misuse or intentional self-use can induce acute poisoning, which has become a common cause of death due to pesticide poisoning [1-3]. Since the first cases of death by PQ poisoning were reported in 1966, the mortality rate has risen to 50-60% [2, 4]. Following PQ poisoning, the lungs are the major target organ for injury, and PQ lung may develop. PQ lung is manifested as acute lung injury (ALI) or adult respiratory distress syndrome in the early stage and as intra-alveolar and interstitial fibrosis in the late stage; being the main cause of death in PO poisoning patients [1]. At present, there are no antidotes or effective therapies for PQ poisoning [2, 3]; therefore, it is imperative to elucidate the underlying mechanism of PQ poisoning for the design of an effective treatment.

Mesenchymal stem cells (MSCs) are those originating from the mesoderm in the early stage of development, and possess a high renewal capability and multi-lineage differentiation potential. MSCs can come from different tissues and organs, including adipose tissue, bone marrow, and cord blood, and are regarded as an ideal cell source for tissue injury diseases [5]. Studies have shown that MSCs administered exogenously can home to injured lung tissues and either play a role in direct repair, by being directly integrated into the injury site, or in lung protection, by transdifferentiating into lung pulmo-

nary alveolar epithelial cells or endothelial cells. In addition, MSCs can participate in the inflammatory reaction and immune regulation of lung injury via the paracrine secretory mechanism [6-9] and antifibrotic capacity [10]. Other studies have suggested that in lipopolysaccharide (LPS)-induced ALI, MSCs can regulate the activity of NF-κB in pulmonary alveolar macrophages, and increase the secretion of interleukin-10 (IL-10), thus relieving inflammation [11, 12]. In further studies using animal models, MSCs have been demonstrated to exert significant protection against inflammation-induced lung injury [13], and can remarkably mitigate the inflammatory reaction of isolated human lungs infected with viable organisms [14].

Mucin (MUC), a large molecular-weight glycoprotein, rich in serine and threonine, encoded by the *MUC* gene, is the main component of airway mucus [15]. MUC mediates the biological characteristics (protective effect) and physical properties (convergence, viscosity, visco-elasticity, and slipping) of mucus. MUC5AC and MUC5B are the major secretory mucins in the airway. MUC5B can protect the airway under normal conditions; however, the autoimmune function of MUC5B-deficient mice is impaired. The immune function can be restored following treatment with a MUC5B promoter variant [16].

Nevertheless, an increase in MUC5B that exceeds the normal range will result in airway injury. A gain-of-function MUC5B promoter variant is the strongest risk factor for idiopathic pulmonary fibrosis (IPF) [17]. MUC5B is significantly increased in PQ poisoning, smoking-induced chronic bronchitis, cystic fibrosis, and primary ciliary dyskinesia [18-20]. The increase in MUC5B is a response to various stimulations including nerve reactions and inflammatory mediators, and is closely related to IL-1β, IL-6, IL-9, IL-13, IL-17, and tumor necrosis factor-α [21-24]. IL-17 not only promotes the expression and secretion of mucins in respiratory tract epithelium but also causes lung injury. Based on some studies, IL-17 has a strong pro-inflammatory effect and can induce several types of cells to release pro-inflammatory cytokines, resulting in excessive inflammatory reactions [25-27]. It has been shown that IL-17 is strongly associated with the occurrence and development of ALI (Zhi-Xin, Mu-Sen et al.).

Here, we hypothesized that MSCs would have a positive impact on PQ-induced pulmonary injury *in vitro*, and *in vivo* using a rat model. The impact of MSCs was analyzed with respect to cytokine response and histopathology of lung mRNA expression levels of selected genes of interest, including *Muc5b*, *IL-6*, and *Il-17*, with a view to investigating the role of muc5b and ERK/MAPK signaling in the improvement of PQ-induced ALI by MSCs.

Materials and methods

Experimental animals

Male Sprague Dawley rats of clean grade (weight: 200-250 g) were provided by the Experimental Animal Center of China Medical University. The rats were acclimated for 1 week with the following housing conditions: 20-25°C, 40-70% humidity, 12 h/12 h dark/light cycle, and free access to food and water. All experimental protocols were approved by the Animal Ethics Committee of Shengjing Hospital of China Medical University.

Rat bone mesenchymal stem cells (BMSCs) and cell culture

Rat MSCs were purchased from Cyagen Bioscience, Inc., (Guangzhou, China), which were derived from normal rat bone marrow. The MSCs expressed CD90, CD44, and CD29, but not CD34, CD45, or CD11b/c, as shown by flow cytometry data supplied by the company (Supplementary Material). The MSCs were grown in SD rat MSC basal medium (Cyagen Bioscience, Inc., Guangzhou, China) supplemented with 10% SD rat MSC-qualified fetal bovine serum, 1% penicillin-streptomycin, and 1% glutamine at 37°C, 5% CO_2, and saturated humidity. The growth medium was changed every two days. At approximately 80-90% confluence, the MSCs were dissociated using trypsin-EDTA and passaged. Lentivirus carrying GFP (pLenO-GFP) was obtained from Cyagen Bioscience, Inc., (Guangzhou, China). The MSCs were infected with pLenO-GFP at aMOI = 50, and cultured on a 6-well plate (10^6 cells/well) at 37°C, 5% CO_2. The infection efficiency of pLenO-GFP was evaluated by fluorescence microscopy 24 h after transfection (Olympus Co., Tokyo, Japan).

Culture of rat pulmonary alveolar type II epithelial (ATII) cells

Rat pulmonary alveolar type II epithelial cells (ATII cells; RAT-iCell-a005) were purchased from iCell Bioscience Inc., (Shanghai, China)

and cultured in PriMed-iCELL-001 culture medium (iCell Bioscience Inc., Shanghai, China) containing 10% FBS at 37°C, 5% CO_2.

MTT assay for cell viability

The cytotoxic effects of PQ on rat ATII cells were assessed using the 3-(4, 5-dimethyl-2-thiazolyl)-2,5-diphenyl-2H-tetrazolium bromide (MTT) assay. The rat ATII cells were seeded onto 96-well plates (5×10^4 cells per well in 100 μL medium) and allowed to adhere. The cells were exposed to different concentrations (0, 10, 50, 100, 500, 1000 μM) of PQ and incubated for 24 h. After the incubation period, 10 μL 0.5 mg/mL MTT was added to each well and incubated for an additional 4 h at 37°C. Subsequently, the supernatant was discarded and 200 μL DMSO was added. The absorbance was measured at 490 nm using a Bio-Tek MQX 680 (Bio-Tek Instruments Inc., Winooski, VT, USA).

Cell grouping

BMSC intervention group (PQ+BMSC): BMSCs were detached after treatment with trypsin-EDTA (1:250) (Gibco, USA) and seeded onto 100-mm cell culture dishes at a concentration of 3-5 × 10^5 cells/well in α-MEM medium supplemented with 10% fetal bovine serum and antibiotics (Gibco, USA). The cells were cultured until 80% confluence was reached, with the culture medium being changed every 48 hours. The 80% confluent cells were cultured for a further 48 hours in ECM basal medium containing 2% FBS, following which, the medium designated "conditioned BMSC medium" was collected, containing ECM, FBS, and any factors secreted by the non-activated BMSCs. The culture medium was centrifuged to remove debris. At 80% confluence, ATII cells were cultured in "conditioned BMSC medium" for a further 48 hours, following which, 100 μmol/L PQ was added as treatment.

PQ group: ATII cells were cultured in PriMed-iCELL-001 culture medium until 80% confluence was reached, following which, 100 μmol/L PQ was added as treatment.

Control group: ATII cells were cultured in PriMed-iCELL-001 culture medium. The levels of IL-6, IL-17, and muc5b in the supernatants were measured using ELISA assays.

Animal grouping and treatment

A solution of 20% PQ was diluted 100 times with physiological saline to a concentration of 2 mg/mL. Thirty rats were randomly divided into three groups: PQ poisoning group (PQ group, n = 10), the PQ poisoning rat model was established by intraperitoneal injection of 20 mg/kg PQ; MSC treatment group (PQ+BMSC) group, n = 10), 1 h after the intraperitoneal injection of PQ, 3 × 10^6 MSCs were injected intraperitoneally; normal control group (control group, n = 10), an equal amount of physiological saline was injected intraperitoneally. Rats were sacrificed 24 h following saline or MSC infusion. Lung lobes were obtained for further analysis.

Lung histopathology

For the evaluation of the severity of lung injury, the right middle lung lobes were obtained 24 h following MSC infusion. The lung tissues were then fixed in 4% paraformaldehyde for 24 h. After fixation, lung tissues were embedded in paraffin and cut into 5-μm sections. Subsequently, the sections were examined by H&E staining. H&E scoring items included edema, congestion, neutrophil infiltration, intratracheal hemorrhage and debris, and cell hyperplasia. Each item was assessed as a score of 0, 1, 2, or 3, and the H&E score was the sum of five item scores [10].

Immunohistochemistry study

The lung sections were preheated at 60°C for 1 hour, followed by dewaxed with xylene, hydration, and washed in 0.01 mol/L of citrate buffer. Inhibiting endogenous peroxidase with 3% H_2O_2 in methanol, and the sections were then incubated with anti-muc5b (Santa Cruz Biotechnology Inc, Texas, USA) and anti-ERK1/2 (Abcam, Cambridge, USA) polyclonal antibodies overnight at 4°C. The sections were incubated with the corresponding secondary antibodies at room temperature for 30 minutes. Reaction products were identified using diaminobenzidine and counterstained with hematoxylin. The positive results were brown-yellow or brown granules distributed on the surface of the bronchial mucosa, alveolar wall, and alveolar septum of lung tissue. The image was generated using the NIS-ElementSF2.30 image acquisition software, and the average optical density

Table 1. The primer sequenc of target genes for RT-PCR

Target Gene	Primer Sequence (5'→3')
Muc5b-F	CACCAACAGTGGGAAGGAAG
Muc5b-R	CACTCAAAGATACGGTCACGC
Bax-F	ATGGAGCTGCAGAGGATTCG
Bax-R	AATGTCCAGCCCATGATGGT
Bcl-F	AGCCTGAGAGCAACCCAATG
Bcl-R	TTCCTTCTTGGGTATGGAAT
Gapdh-F	AAGGGTGGGGACAAGACAGT
Gapdh-R	AAGTTGTCCGGAGGTGCTAA

(OD) of the positive area was analyzed using the Image-Pro-Plus software.

Detection of indicators in bronchoalveolar lavage fluid (BALF)

At 24 h after the intraperitoneal injection of MSCs, the rats were sacrificed and the trachea and primary bronchus were dissected. Tracheal intubation was performed, and the left lung was lavaged three times with 0.5 mL precooled PBS. BALF was collected and centrifuged for 10 min at 4°C, 1,500 × g. The protein content in BALF was measured with a protein quantitation kit (Bio-Rad, USA) according to the manufacturer's instructions. The concentrations of IL-17, IL-6, and MUC5B in BALF were measured by ELISA according to the manufacturer's instructions (Abcam, Cambridge, UK).

Measurement of the wet/dry weight (W/D) of the lungs

The right upper lung lobe was collected, the wet weight (W) was taken following removal of the water and blood from the surface using filter paper, and the dry weight (D) was taken 24 h after drying at 80°C. The W/D ratio of the lung tissues was subsequently calculated.

RNA-seq data analysis

RNA-seq was performed by Genesky Bio-Tech Co. Ltd (Shanghai, China). The RNA sequencing libraries were constructed from the RNA extracted and amplified using the standard Illumina library prep protocols. RNA-seq was performed on an Illumina HiSeq 2500 or above platform using the 150 bp PE protocol. Raw sequencing reads were evaluated using FastQC (Version 0.11.4) (http://www.bioinformatics.babraham.ac.uk/projects/fastqc/), followed by trimmedbytrim_galore (Version 0.3.3) (http://www.bioinformatics.babraham.ac.uk/projects/trim_galore/) to remove the primers and low-quality (Q < 10) sequences. Clean reads were aligned with the rat genome using TopHat [28, 29] (Version 2.1.0) with at most two mismatches. Only the uniquely mapped reads were retained for further analysis in the present study. The statistics of raw reads, clean reads, and mapped reads are summarized. Read distribution over the gene structure, and other quality evaluation of mapped reads, were analyzed using RNA-SeQC [30] (Version 1.1.8). For each transcript, Fragments Per Kilobase of transcript per Million mapped reads (FPKM) calculated by Cufflinks [31] (Version 2.2.1) with default parameters were used to evaluate the expression levels. Comparison of the total gene expression profiles of three samples was performed using principal components analysis (PCA). The differentially expressed (DE) genes were identified by Cuffdiff [32, 33] (Version 2.2.1) with more than one-fold expression change at an FDR-adjusted *p*-value of 0.05. In addition, alternative splicing (AS) events of three samples were extracted and compared using the Macs tool [34]. Novel transcripts in the present study were predicted by Cufflinks [35] (Version 2.2.1). Fusion genes of each sample were detected by FusionMap [36], and then filtered with the most stringent recommended criteria.

Quantitative real-time PCR

Total RNA was extracted from lung tissues using the RNeasy Mini kit (Qiagen, CA, USA), and the quality and quantity of the obtained RNA was assessed spectrophotometrically. Equal amounts of RNA were reverse-transcribed into cDNA using the Quanti-Tect Reverse Transcription kit (Qiagen, CA, USA) according to the manufacturer's instructions. To assess the expression of target genes, quantitative real-time PCR was performed using the Rotor-Gene SYBR Green PCR kit (Qiagen, CA, USA) with the Rotor-Gene Q system (Qiagen, CA, USA). *β-Actin* (*Actb*) was used as a reference housekeeping gene. The sense and antisense primers are shown in **Table 1**. PCR reactions included a 5-min enzyme activation at 95°C, followed by 40 cycles at 95°C for 5 sec (denaturing) and 60°C for 10 sec (annealing/extension). The changes in target gene expression were calculated using the comparative CT (ΔΔCT, thresh-

old cycle) method and are presented as the fold change using the 2-ΔΔCT formula.

Detection of ERK1/2 protein expression in lung tissues by western blotting

The total protein concentration was measured using a BCA Protein Assay kit (Beyotime, Shanghai, China). For western blotting, 30 μg protein was loaded into each lane of 10% SDS-PAGE gels, followed by electrophoresis and protein transfer to PVDF membranes (Millipore). Following transfer, the membranes were blocked with 5% BSA in PBST. Immunoblots were probed with primary antibody at 4°C overnight, followed by secondary antibodies (ZSGB-BIO, Beijing, China, 1:5000 dilution) for 30 min at room temperature. After extensive washing with PBST, the membranes were incubated in ECL reagent (Millipore) for HRP detection, and subsequently exposed to autoradiography film (Bio-Rad, Co., Ltd, USA) for band visualization. GAPDH was used as a loading control. The relative amounts of various proteins were analyzed, and the results were quantitated using the Image J software.

Measurement of mitochondrial membrane potential (MMP)

An ATII cell suspension containing 10^6 cells was collected by digestion with trypsin-EDTA and centrifuged at 1,000 rpm for 5 min. Cells were washed twice with precooled PBS and centrifuged at 1,000 rpm for 5 min each time. A volume of 0.5 mL JC-1 stain (Beijing Solarbio Biotechnology Co. Ltd., China) was added to the cells and mixed evenly, followed by incubation at 37°C for 20 min and centrifugation at 1,000 rpm for 5 min. Subsequently, the cells were washed three times with JC-1 staining buffer, resuspended, and detected by flowcytometry. The excitation and emission wavelengths of the JC-1 monomer and polymer were 490 nm and 530 nm and 525 nm and 590 nm, respectively. The data were analyzed using the CellQuest software.

Detection of apoptotic ATII cells

After reaching confluence, the ATII cells were treated with DMSO (1 M, as the control group), paraquat (100 μM), or medium, alone or in combination, for 24 h. After treatment, ATII cells were resuspended in annexin V binding buffer and stained with annexin V-FITC and propidium iodide (PI) (1 g/mL) using the Annexin V-FITC Apoptosis Detection kit (Beijing Solarbio Biotechnology Co. Ltd., China) according to the manufacturer's instructions. After incubation at room temperature, the apoptotic cells were quantitated by flow cytometry (BD Bioscience, Franklin Lakes, NJ, USA). Early apoptosis is defined by annexin V+/PI staining (lower right quadrant, LR), and late apoptosis is defined by annexin V+/PI+ staining (upper right quadrant, UR).

Detection of caspase-3 activity in lung tissue

Caspase-3 protease activity in the lung tissue was determined using the Caspase-3 Colorimetric Assay kit (Sigma-Aldrich; Merck KGaA), in accordance with the manufacturer's protocol. In brief, following homogenization of whole lung tissue in cell lysis buffer, homogenates were centrifuged for 1 min at 10,000 × g, and the supernatant was extracted and incubated with Asp-Glu-Val-Asp-p-nitroanilide (pNA) in reaction buffer for 90 min at 37°C. Levels of the chromophore pNA were quantitated using a spectrophotometer at 405 nm, which reflected the caspase-3 activity. Data were normalized to the lung weight.

Statistical analysis

The SPSS 16.0 statistical software was used for analysis. All data are presented as the mean ± standard deviation (mean ± SD). The intergroup comparison was performed by one-way ANOVA. $P < 0.05$ suggested that a difference was statistically significant.

Results

Isolation and characterization of BMSCs

Proliferation of BMSCs accelerated significantly after six generations. Lentivirus transfection (MOI = 50) did not affect the proliferation or morphology of BMSCs. The GFP-positive cells were greater than 80% by counting under fluorescence microscopy (**Figure 1A**, **1B**). Fluorescence was measured in the lung 24 h after BMSC administration using fluorescence microscopy. As shown in **Figure 1C**, **1D**, fluorescence was distributed throughout the distal lungs.

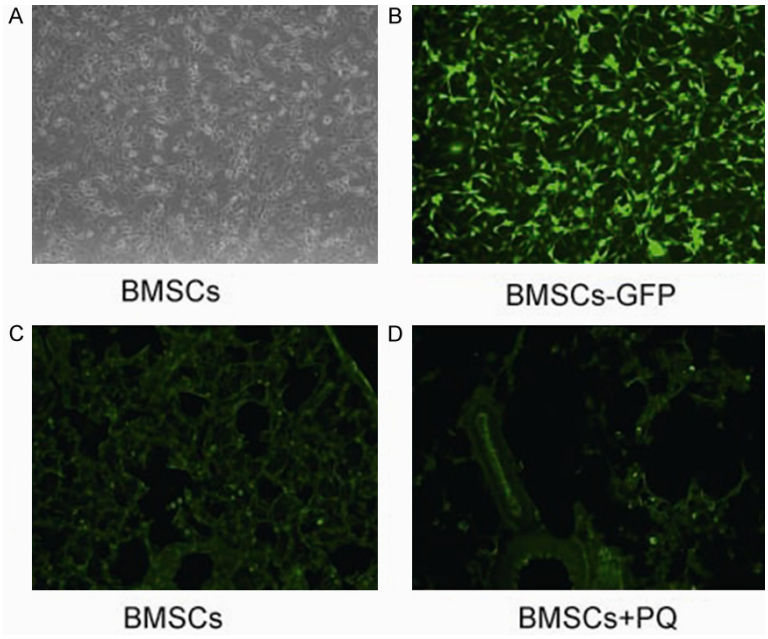

Figure 1. Isolation and characterization of BMSCs. BMSCs carrying GFP were observed by fluorescence microscopy. The transfection efficiency was over 80% (A, B). 24 hours after BMSC administration, the distribution of BMSC fluorescence was observeded throughout the distal lungs. (C) Normal control group; (D) PQ group.

BMSCs ameliorate ALI in a PQ-induced animal model

H&E staining: The observations under light microscopy showed that the lung tissues had a normal structure, a clear alveolar morphology, and no congestion or edema in the control group. In the PQ group, there was a damaged alveolar structure, alveolar bleeding, pulmonary interstitial congestion and edema, a large number of inflammatory cells, and lung injury worsened over time. In the PQ+BMSC group, lung injury was significantly improved as compared with the PQ group (**Figure 2A-C**). There was a statistical difference in the lung injury score among the three groups ($P < 0.05$, **Figure 2D**).

Lung W/D ratio

Lung edema was determined using the lung weight ratio. When compared with that of the control group, the lung W/D ratio was significantly increased in the PQ group, and that in the PQ+BMSC group was markedly decreased as compared with that of the PQ group ($P < 0.05$, **Figure 2E**).

BMSCs decrease muc5b in a PQ-induced animal model

Heatmaps: To elucidate the molecular mechanisms underlying the effects of MSCs on ALI induced by PQ, whole transcriptome analysis of the rat lung in the PQ group (n = 3), the control group (n = 3), and the PQ+BMSC group (n = 3) was performed using RNA-seq. The gene expression analysis revealed differential expression of several mRNAs in the PQ group as compared with the control and PQ+BMSC groups. We found that the expression of *MUC5B* was remarkably increased in the PQ group, and the expression of *MUC5B* was evidently decreased in the PQ+BMSC group, indicating that *MUC5B* play an important role in the occurrence of PQ-induced lung injury (**Figure 3A**).

Quantitative reverse transcription PCR: Using quantitative real-time PCR, we found that in comparison with the control group, the mRNA expression of *MUC5B* in lung tissues was significantly increased in the PQ group; and in comparison with the PQ group, the mRNA expression of *MUC5B* was markedly decreased in the PQ+BMSC group ($P < 0.05$, **Figure 3B**), which is consistent with the sequencing results.

ELISA with BALF: ELISA results showed that the levels of MUC5B in BALF from rats in the PQ group were all significantly higher than those in the control group; however, these levels in the PQ+BMSC group were all markedly reduced as compared with those in the PQ group ($P < 0.05$; **Figure 3C**).

ELISA with ATII culture medium: The effects of PQ on ATII cell viability were analyzed by exposing ATII cells to different concentrations of PQ for 24 hours. Analysis of the MMT assay results showed that the ability of ATII cells to survive PQ exposure was concentration-dependent (**Figure 3D**). After a 24-hour incubation with 100 μM PQ, the number of viable cells was reduced by approximately 25%. The optimum

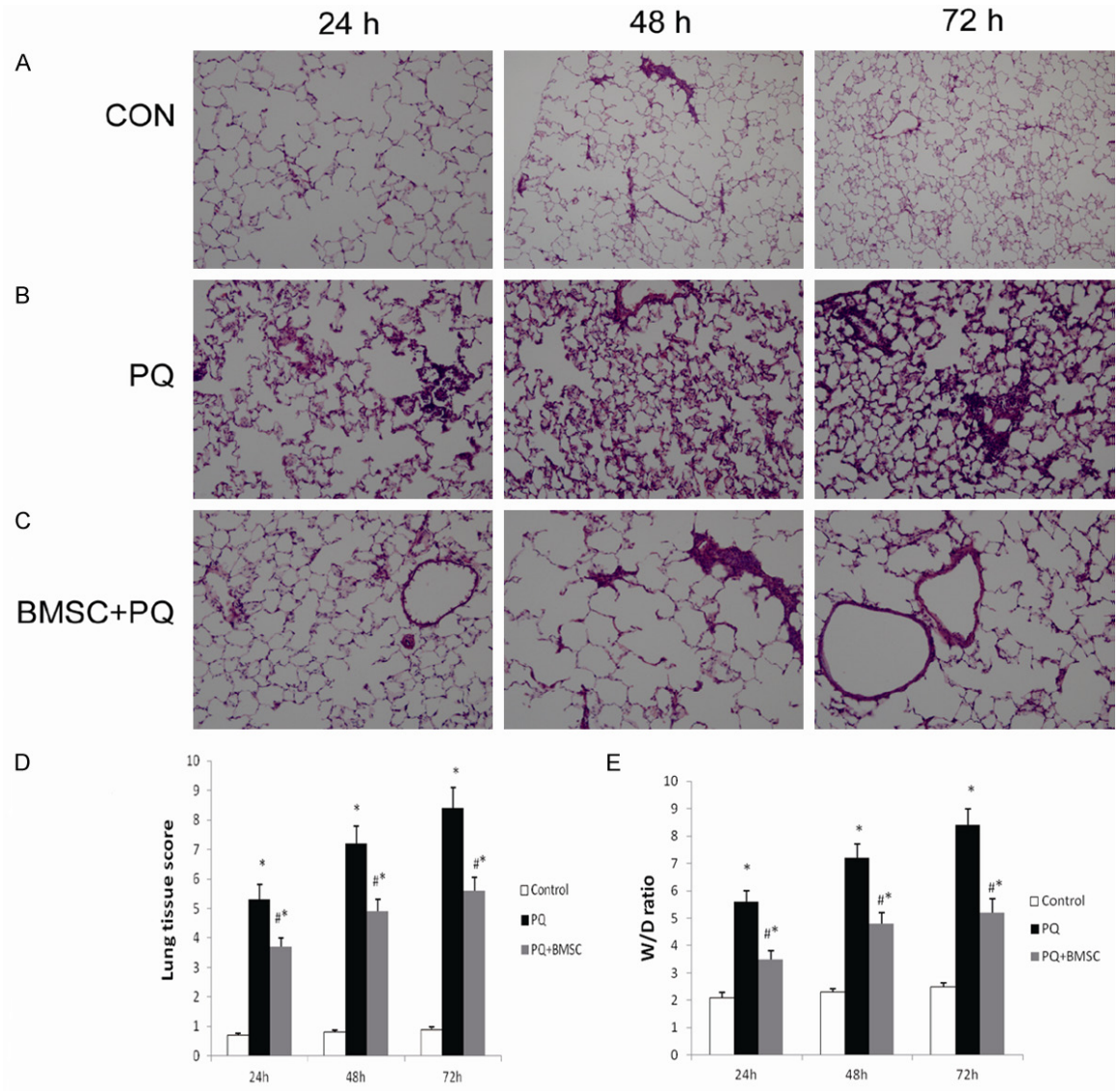

Figure 2. BMSCs ameliorated the histopathological changes in lung tissues of rats with PQ-induced ALI. Lung tissues were fixed in 10% formalin, sectioned, and stained with H&E (200 ×). Photomicrograph of lung tissue from the control group (A). Photomicrograph of lung tissue from the PQ group (B). Photomicrograph of lung tissue from the PQ+BMSC group (C). Histopathological scoring of lung injury in the three groups (D). BMSCs reduced the lung W/D ratio in rats with PQ-induced ALI (E). Data are presented as the mean ± SD, n = 10. $^{*}P < 0.05$ as compared with control rats; $^{\#}P < 0.05$ as compared with rats with PQ.

concentration of PQ was chosen for use in further experiments. To confirm whether BMSCs affected the secretion of Muc5B from ATII cells, ATII cells were pretreated with PQ for different time periods. ELISA results showed that the protein levels of MUC5B in the cell culture medium were significantly higher in the PQ group than in the control group, and were evidently lower in the PQ+BMSC group than in the PQ group ($P < 0.05$; **Figure 3E**).

Immunohistochemistry staining of Muc5b in lung tissue: In lung tissue, the expression of mucin Muc5b as brown granules is localized to the bronchial mucosa and alveolar septum. In the control group, a small number of brown granules were identified; however, in the PQ group, these granules were dramatically increased. In the PQ+BMSC group, the expression of mucin Muc5b was decreased significantly as compared with the PQ group ($P <$

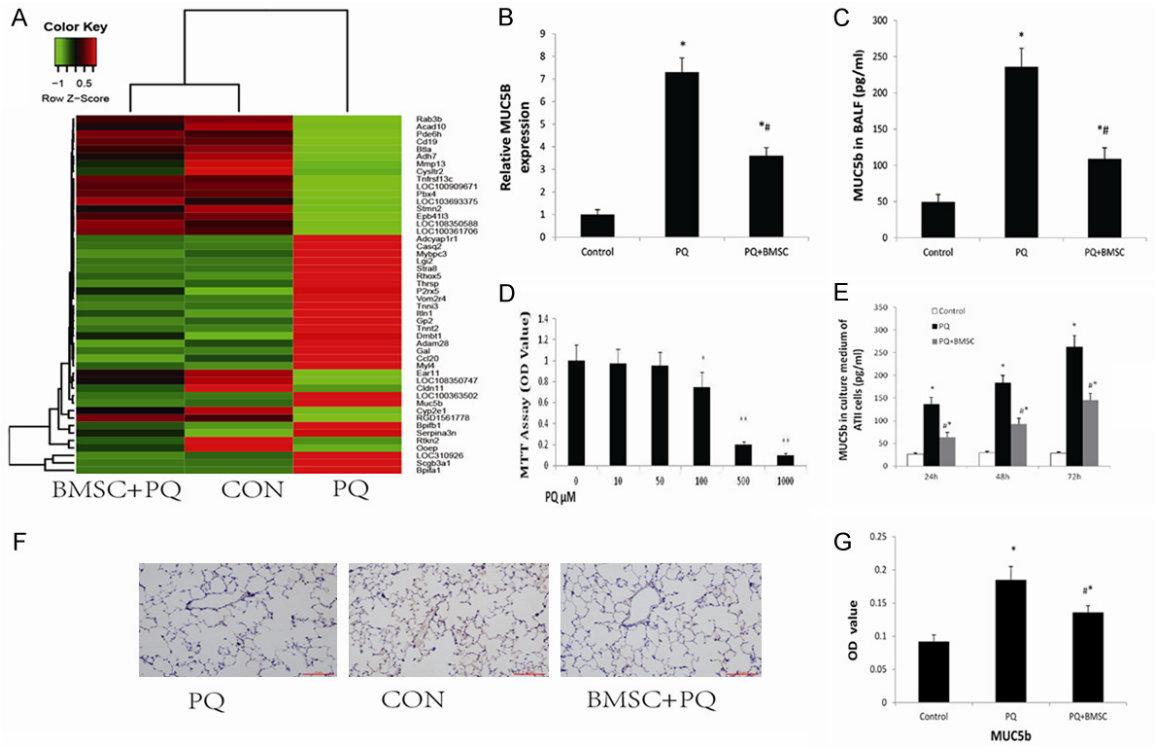

Figure 3. BMSCs decreased the mRNA expression of *muc5b* in the lung tissue of rats with PQ-induced ALI as shown by whole transcriptome analysis (A). Data are presented as the mean ± SD, n = 3. **P* < 0.05 as compared with control rats; #*P* < 0.05 as compared with rats with PQ. BMSCs reduced the mRNA expression of *muc5b* in the lung tissue of rats with PQ-induced ALI as shown by RT-qPCR (B). BMSCs inhibited the concentration of Muc5b in the BALF of rats with PQ-induced ALI using ELISA (C). Effect of PQ on ATII cell viability as examined by the MTT assay (D). BMSCs decreased the concentration of Muc5b in ATII cell culture medium following the administration of PQ by ELISA (E). Immunohistochemistry staining of Muc5b in lung tissue from the control group, the PQ group, and the PQ+BMSC group. 3,3'-diaminobenzidine 4-HCl was used as a chromogen to stain the cells of interest (brown), and a hematoxylin counterstain (blue) was used for background staining. (F) Muc5b immunostaining at 200 × magnification, (G) Changes in OD values in lung with positive expression. Data are presented as the mean ± SD, n = 10. **P* < 0.05 as compared with control rats; #*P* < 0.05 as compared with rats with PQ.

0.05; **Figure 3F**). Semi-quantitative analysis was applied to show the significant difference as *P* < 0.05, **Figure 3G**.

BMSCs inhibit apoptosis in ATII cells

Annexin V/PI staining: The cell apoptosis rate in the control, PQ, and PQ+BMSC groups was 6.2±0.3%, 15.6±0.67%, and 10.2±0.36%, respectively; and the percentage of living cells was 93.5±2.87%, 84.6±3.97%, and 88.7±3.52%, respectively. In comparison with the PQ group, the PQ-induced cell apoptosis was reduced, and the percentage of living cells was increased, in the PQ+BMSC group (**Figure 4A**; *P* < 0.05).

Mitochondrial membrane potential assay: As shown by JC-1 staining, the percentage of depolarized L02 cells was 64.7±0.25% in the control group, 73.5±0.58% in the PQ group, and 69.1±0.26% in the PQ+BMSC group. These findings indicate that BMSCs can reduce the early cell apoptosis rate in PQ poisoning. There was a statistically significant difference among the three groups (*P* < 0.05; **Figure 4B**).

Apoptosis-related protein changes: Bcl-2 is known to exert anti-apoptotic effects. We found that the expression of *Bcl-2* mRNA was decreased in the PQ group as compared with the control group, whereas the *Bcl-2* expression was increased in the PQ+BMSC group as compared with the PQ group (*P* < 0.05; **Figure 4C**).

Bax is an important apoptosis gene. We found that the expression of *Bax* mRNA was increased in the PQ group as compared with the control group, whereas the *Bax* expression was decreased in the PQ+BMSC group as compared with the PQ group (*P* < 0.05; **Figure 4D**).

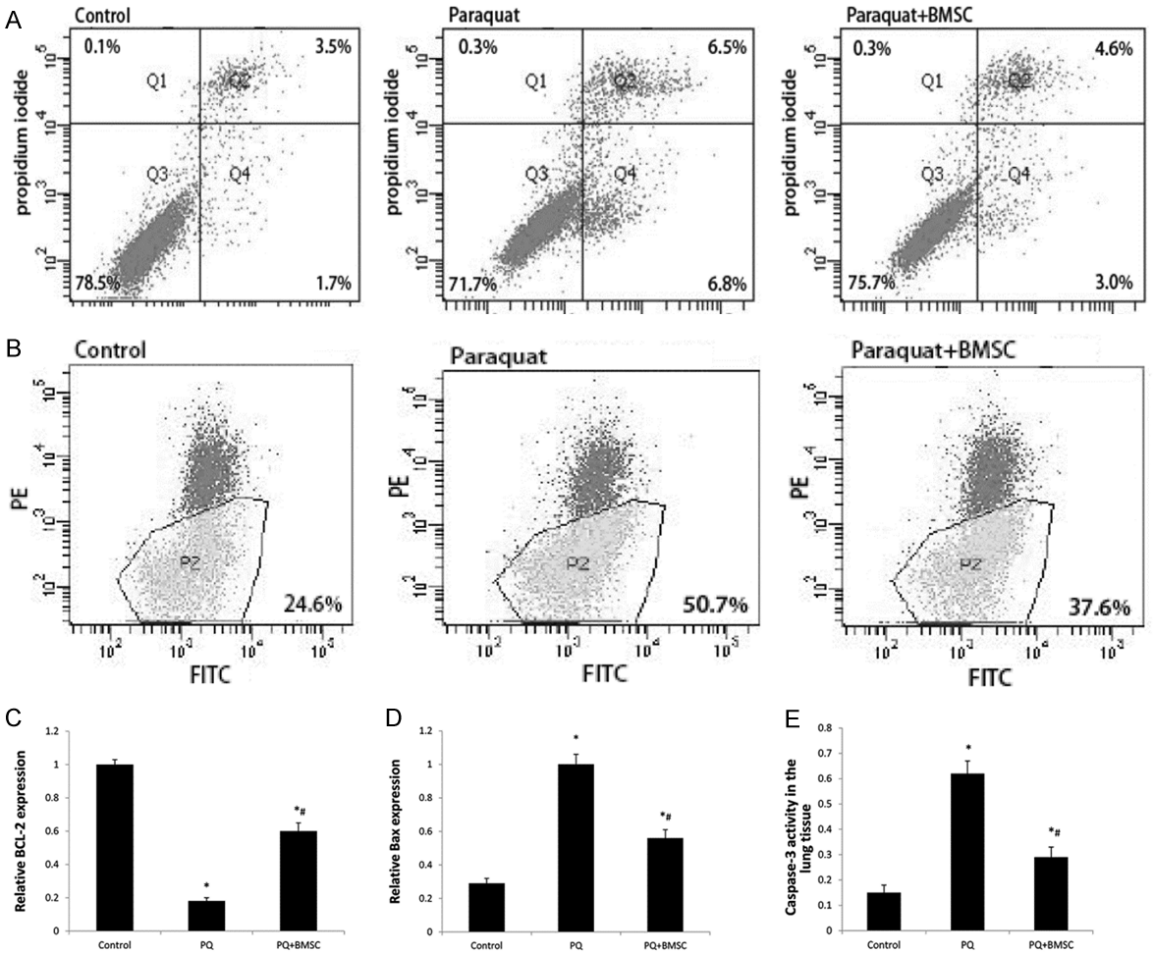

Figure 4. BMSCs decreased the cell apoptosis rate of ATII cells following PQ administration by flowcytometry (A). BMSCs decreased the mitochondrial membrane potential in ATII cells following PQ administration by flowcytometry (B). BMSCs increased *Bcl-2* mRNA expression in the lung tissue of rats with PQ-induced ALI by RT-qPCR (C). BMSCs decreased *Bax* mRNA expression in the lung tissue of rats with PQ-induced ALI by RT-qPCR (D). BMSCs decreased the percentage of caspase-3 activity in rats with PQ-induced ALI using the Caspase-3 Colorimetric Assay kit (E). Data are presented as the mean ± SD, n = 10. **P* < 0.05 as compared with control rats; #*P* < 0.05 as compared with rats with PQ.

Caspase-3 activity in lung tissue: The caspase-3 activity in lung tissue was 0.15 in the control group; however, the proportion was increased to 0.62 in the PQ group. In the PQ+BMSC group, the caspase-3 activity in lung tissue was decreased to 0.29 (*P* < 0.05; **Figure 4E**).

BMSCs reduce inflammation

ELISA with BALF: ELISA results showed that the levels of IL-6 and IL-17 and the protein content in BALF from rats in the PQ group were all significantly higher than those in the control group; however, these levels in the PQ+BMSC group were all markedly reduced as compared with those in the PQ group (*P* < 0.05; **Figure 5A-C**).

ELISA with ATII culture medium: ELISA results showed that the protein levels of IL-6 and IL-17 in the cell culture medium were significantly higher in the PQ group than in the control group, and were evidently lower in the PQ+BMSC group than in the PQ group (*P* < 0.05; **Figure 5D**, **5E**).

BMSCs attenuate ERK1/2 activation in rats with PQ-induced acute lung injury: There was a marked increase in phospho-ERK1/2 in PQ-injured lung tissues. Treatment with BMSCs attenuated this increase in phospho-ERK1/2 as compared with the PQ-treated group (*P* < 0.05; **Figure 6A**, **6B**).

Immunohistochemistry staining of ERK1/2 in lung tissue: In lung tissue, the expression of

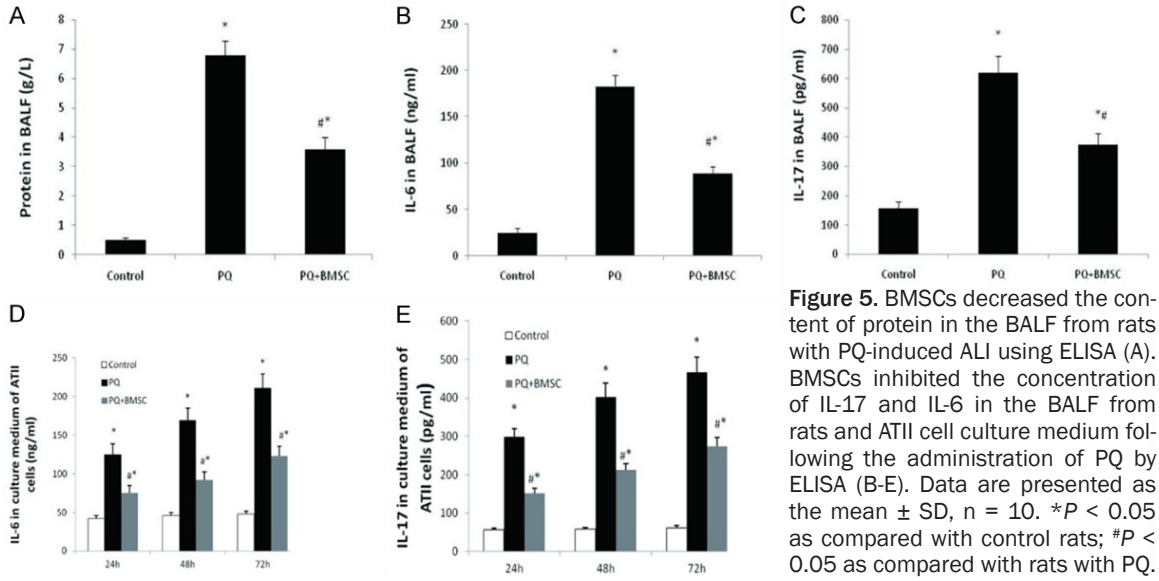

Figure 5. BMSCs decreased the content of protein in the BALF from rats with PQ-induced ALI using ELISA (A). BMSCs inhibited the concentration of IL-17 and IL-6 in the BALF from rats and ATII cell culture medium following the administration of PQ by ELISA (B-E). Data are presented as the mean ± SD, n = 10. **P* < 0.05 as compared with control rats; #*P* < 0.05 as compared with rats with PQ.

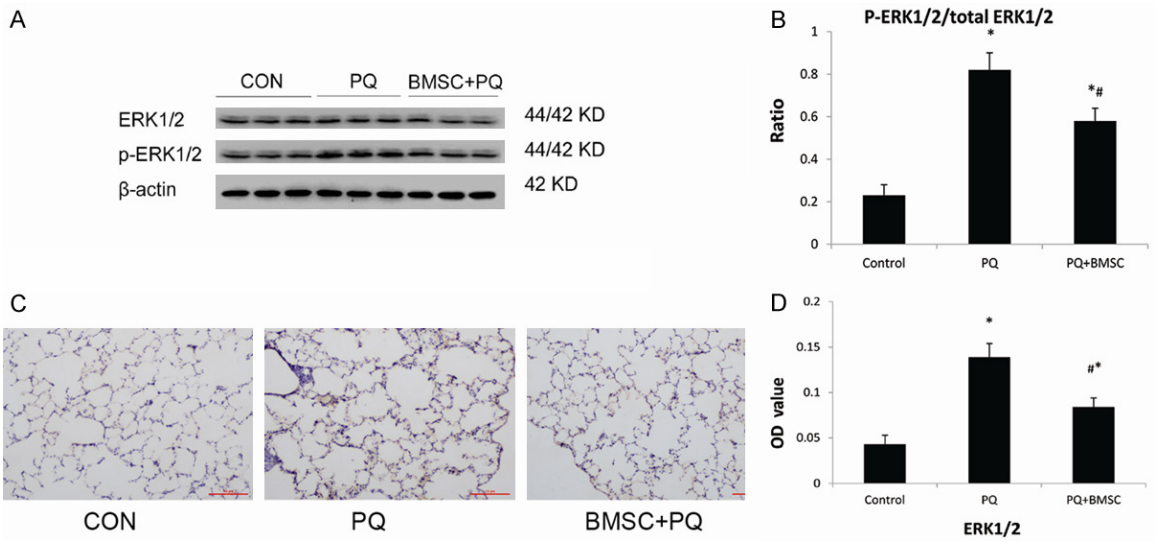

Figure 6. BMSCs attenuated ERK1/2 activation in PQ-induced ALI tissue by western blotting. (A) Expression of ERK1/2 and p-ERK1/2 proteins in lung tissue; (B) p-ERK1/2/total ERK1/2 ratio. Immunohistochemistry staining of ERK1/2 in lung tissue from the control group, the PQ group, and the PQ+BMSC group. 3,3'-diaminobenzidine 4-HCl was used as a chromogen to stain the cells of interest (brown), and a hematoxylin counterstain (blue) was used for background staining. (C) ERK1/2 immunostaining at 200 × magnification, (D) Changes in OD values in lung with positive expression. Data are presented as the mean ± SD, n = 10. **P* < 0.05 as compared with control rats; #*P* < 0.05 as compared with rats with PQ.

ERK1/2 is seen as brown granules. In the control group, a small number of brown granules were identified; however, in the PQ group, these granules were dramatically increased. In the PQ+BMSC group, the expression of ERK1/2 decreased significantly as compared with the PQ group ($P < 0.05$; **Figure 6C**). Semi-quantitative analysis was applied to show the significant difference as $P < 0.05$, **Figure 6D**.

Discussion

To date, many studies have shown that stem cell transplantation has a protective effect on lung injury. Such protection is reflected by two aspects: 1) the implanted stem cells can differentiate into the major pulmonary cells (alveolar epithelial cells and vascular endothelial cells) to play a role in the repair of injured tis-

sues [37]; and 2) the implanted stem cells play an anti-inflammatory role and can protect and maintain the integrity of pulmonary cells [38, 39]. In the present study, we investigated the possible effects of BMSCs on acute lung injury *in vitro*, and *in vivo* using a rat model. Our results show that BMSCs effectively improved alveolar destruction and inhibited apoptosis. BMSCs remarkably inhibited IL-17 and IL-6 production both *in vitro* and *in vivo*, indicating that BMSCs attenuated PQ-induced acute lung injury and improved pulmonary function, in part, via the inhibition of inflammation. In addition, we demonstrate that BMSCs targeted the ERK/MAPK signaling pathway to downregulate inflammatory cell recruitment and goblet cell hyperplasia, leading to the inhibition of inflammation and MUC5B hypersecretion.

Some studies have suggested that in PQ poisoning, ATII cells can actively absorb PQ via the polyamine transport system [40, 41], and the concentration of PQ in lung tissues was shown to be 10-20 times that in the plasma. The toxicity of PQ is directly related to the PQ concentration [42, 43]. PQ induces pulmonary alveolar epithelial cells to produce reactive oxygen species (ROS), and thus causes a serious inflammatory reaction by activating neutrophils and macrophages [44]. The inflammatory cytokines, IL6 and IL17, have been implicated in the pathogenesis of PQ-induced lung injury [45]. IL-6, as the major regulatory factor for the differentiation of inflammatory cells, is secreted by activated macrophages, lymphocytes, and epithelial cells. IL-6 not only promotes the expression of intercellular adhesion molecule-1 but also the differentiation and inflammatory activation of lymphocytes, further enhancing the inflammatory injury reaction. In addition, IL-6 can also promote the respiratory burst and degranulation of neutrophils and stimulate hepatocytes to produce acute-phase proteins, thus causing a serious systematic inflammatory reaction [46].

IL-17, as a pro-inflammatory cytokine, can promote the recruitment and activation of neutrophils at inflammatory sites in the lungs and airway, leading to the secretion of several inflammatory cytokines. It has been proven that IL-17 is associated with many lung diseases such as asthma, sepsis, chronic obstructive pulmonary disease, pulmonary tuberculosis, and lung cancer [47-50]. The present study demonstrates that the levels of IL-6 and IL-17 were significantly increased in the BALF and culture medium in the PQ group, indicating that several effector cells and inflammatory mediators are involved in PQ-induced ALI. Moreover, it was found that the protein content in BALF and the W/D ratio of lung tissues were both increased in the PQ group, suggesting that the permeability of endothelial cells and the water content in the lungs were increased. H&E staining showed pulmonary interstitial congestion and edema, as well as apparent infiltration of inflammatory cells. BMSC treatment could suppress this increase in permeability and the inflammatory reaction of the lung tissues, thus relieving pneumonedema and pulmonary parenchyma injury, which demonstrates lung protection in rats with PQ-induced ALI.

To clarify the underlying mechanism of the protection against PQ-induced ALI by BMSCs, we conducted second-generation sequencing of lung tissues, showing that the *MUC5B* level was significantly increased in the PQ group but remarkably decreased in the PQ+BMSC group. In the normal airway, Muc5B is mainly expressed in mucus cells of the submucosal gland [51, 52]; however, the product of the *MUC5* gene is also present in the superficial epithelium of the affected airway (e.g., cystic fibrosis or asthma) [53, 54]. MUC5B expression may be attributed to goblet cell hyperplasia and an increase in mucus secretion caused by several airway diseases [55]. In the diseased airway epithelium, both IL-6 and IL-17 are involved in the induction of expression of the Mucin 5B gene, likely via the Jak2/STAT3 and ERK1/2 signaling pathways [56, 57]. It has been reported that activation of ERK1/2 signaling can stabilize the mRNA of IL-17 downstream target genes [58, 59]. The present study also shows that when ERK1/2 protein expression in lung tissues was increased in the PQ group, MUC5B expression was upregulated and the IL-17 level in BALF and culture medium was increased. In the PQ+MSC group, ERK1/2 protein expression was significantly decreased, MUC5B expression was downregulated, and the IL-17 level in BALF and culture medium was reduced.

As PQ poisoning happens, upregulated ERK1/2 expression in lung tissues is related to the induction of ROS production in pulmonary alve-

olar epithelial cells. Several *in vitro* studies have confirmed that cell apoptosis is accompanied by a decrease in mitochondrial membrane potential and mitochondrial quality; thus, some scholars believe that ERK1/2 activation is a necessary condition for mitochondrial membrane depolarization and cell apoptosis. Following activation by phosphorylation, the ERK1/2 pathway can continuously activate downstream proteins, including the Bcl-2 family, which play an important regulatory role in the signal transduction of cell apoptosis, for example, a Bax/Bcl-2 proportional imbalance can cause a change in mitochondrial membrane potential in cells and the release of mitochondrial Cytochrome C into the cytoplasm, followed by the activation of caspase-3, eventually resulting in apoptosis [60-62]. The present study shows that when PQ acted on rat ATII cells, the ERK1/2 pathway was activated, the mitochondrial membrane potential was decreased, and there was an increase in the cell apoptosis rate and the expression levels of the apoptosis-related caspase-3 and the pro-apoptosis Bax proteins, but a decrease in the expression level of the anti-apoptosis Bcl-2 protein. These findings suggest that PQ causes an increase in cell apoptosis via the ERK1/2 signaling pathway, which is in accordance with the results reported in the literature [63, 64]. Following BMSC treatment, the mitochondrial membrane potential in ATII cells was restored, the cell apoptosis rate was decreased, and there was a decrease in the expression levels of caspase-3 and Bax but an increase in the expression level of Bcl-2; and as a result, PQ-induced ATII cell apoptosis was suppressed.

In summary, our results suggest that BMSC treatment demonstrates protection against PQ-induced lung injury in rats, and the underlying mechanism may be inhibition of the MUC5B and ERK/MAPK signaling pathways, thus improving the endothelial permeability and reducing the inflammatory reaction and cell apoptosis in vivo and in vitro, further alleviating lung injury. The present study provides a theoretical basis for the clinical treatment of PQ with BMSCs.

Acknowledgements

The present work was funded in part by the National Key Clinical Specialist Fund (2012-649), China. We would like to thank all the individuals who helped us to carry out this work.

Disclosure of conflict of interest

None.

Address correspondence to: Dr. Min Zhao, Department of Emergency, Shengjing Hospital Affiliated to China Medical University, No. 36 Sanhao Street, Heping District, Shenyang 110004, Liaoning Province, China. E-mail: zhaomsy@163.com

References

[1] Dinis-Oliveira RJ, Duarte JA, Sanchez-Navarro A, Remiao F, Bastos ML and Carvalho F. Paraquat poisonings: mechanisms of lung toxicity, clinical features, and treatment. Crit Rev Toxicol 2008; 38: 13-71.

[2] Gunawardena G, Roberts DM and Buckley NA. Randomized control trial of immunosuppression in paraquat poisoning. Crit Care Med 2007; 35: 330-331.

[3] Gawarammana IB and Buckley NA. Medical management of paraquat ingestion. Br J Clin Pharmacol 2011; 72: 745-757.

[4] Bullivant CM. Accidental poisoning by paraquat: report of two cases in man. Br Med J 1966; 1: 1272-1273.

[5] Walter J, Ware LB and Matthay MA. Mesenchymal stem cells: mechanisms of potential therapeutic benefit in ARDS and sepsis. Lancet Respir Med 2014; 2: 1016-1026.

[6] Dimitriou R, Tsiridis E and Giannoudis PV. Current concepts of molecular aspects of bone healing. Injury 2005; 36: 1392-1404.

[7] Sotnikova NV, Stavrova LA, Gur'antseva LA, Khrichkova TY, Fomina TI, Vetoshkina NV, Dubskaya TY, Sergeeva SA, Epshtein OI, Ermolaeva LA, Dygai AM and Gol'dberg ED. Mechanisms of the effects of granulocytic CSF on tissue reparation during chronic CCl4-induced damage to the liver. Bull Exp Biol Med 2005; 140: 644-647.

[8] Aggarwal S and Pittenger MF. Human mesenchymal stem cells modulate allogeneic immune cell responses. Blood 2005; 105: 1815-1822.

[9] Yagi H, Soto-Gutierrez A, Parekkadan B, Kitagawa Y, Tompkins RG, Kobayashi N and Yarmush ML. Mesenchymal stem cells: mechanisms of immunomodulation and homing. Cell Transplant 2010; 19: 667-679.

[10] Li L, Zhang Y, Li Y, Yu B, Xu Y, Zhao S and Guan Z. Mesenchymal stem cell transplantation attenuates cardiac fibrosis associated with isoproterenol-induced global heart failure. Transpl Int 2008; 21: 1181-1189.

[11] Gupta N, Su X, Popov B, Lee JW, Serikov V and Matthay MA. Intrapulmonary delivery of bone marrow-derived mesenchymal stem cells improves survival and attenuates endotoxin-induced acute lung injury in mice. J Immunol 2007; 179: 1855-1863.
[12] Nemeth K, Leelahavanichkul A, Yuen PS, Mayer B, Parmelee A, Doi K, Robey PG, Leelahavanichkul K, Koller BH, Brown JM, Hu X, Jelinek I, Star RA and Mezey E. Bone marrow stromal cells attenuate sepsis via prostaglandin E(2)-dependent reprogramming of host macrophages to increase their interleukin-10 production. Nat Med 2009; 15: 42-49.
[13] Rojas M, Xu J, Woods CR, Mora AL, Spears W, Roman J and Brigham KL. Bone marrow-derived mesenchymal stem cells in repair of the injured lung. Am J Respir Cell Mol Biol 2005; 33: 145-152.
[14] Wu GD, Bowdish ME, Jin YS, Zhu H, Mitsuhashi N, Barsky LW and Barr ML. Contribution of mesenchymal progenitor cells to tissue repair in rat cardiac allografts undergoing chronic rejection. J Heart Lung Transplant 2005; 24: 2160-2169.
[15] Rubin BK, Priftis KN, Schmidt HJ and Henke MO. Secretory hyperresponsiveness and pulmonary mucus hypersecretion. Chest 2014; 146: 496-507.
[16] Molyneaux PL, Cox MJ, Willis-Owen SA, Mallia P, Russell KE, Russell AM, Murphy E, Johnston SL, Schwartz DA, Wells AU, Cookson WO, Maher TM and Moffatt MF. The role of bacteria in the pathogenesis and progression of idiopathic pulmonary fibrosis. Am J Respir Crit Care Med 2014; 190: 906-913.
[17] Hunninghake GM, Hatabu H, Okajima Y, Gao W, Dupuis J, Latourelle JC, Nishino M, Araki T, Zazueta OE, Kurugol S, Ross JC, San Jose Estepar R, Murphy E, Steele MP, Loyd JE, Schwarz MI, Fingerlin TE, Rosas IO, Washko GR, O'Connor GT and Schwartz DA. MUC5B promoter polymorphism and interstitial lung abnormalities. N Engl J Med 2013; 368: 2192-2200.
[18] Kirkham S, Sheehan JK, Knight D, Richardson PS and Thornton DJ. Heterogeneity of airways mucus: variations in the amounts and glycoforms of the major oligomeric mucins MUC5AC and MUC5B. Biochem J 2002; 361: 537-546.
[19] Henderson AG, Ehre C, Button B, Abdullah LH, Cai LH, Leigh MW, DeMaria GC, Matsui H, Donaldson SH, Davis CW, Sheehan JK, Boucher RC and Kesimer M. Cystic fibrosis airway secretions exhibit mucin hyperconcentration and increased osmotic pressure. J Clin Invest 2014; 124: 3047-3060.
[20] Monte AA, Sun H, Rapp-Olsson AM, Mohamed F, Gawarammana I, Buckley NA, Evans CM, Yang IV and Schwartz DA. The plasma concentration of MUC5B is associated with clinical outcomes in paraquat-poisoned patients. Am J Respir Crit Care Med 2018; 197: 663-665.
[21] Williams OW, Sharafkhaneh A, Kim V, Dickey BF and Evans CM. Airway mucus: from production to secretion. Am J Respir Cell Mol Biol 2006; 34: 527-536.
[22] Kufe DW. Mucins in cancer: function, prognosis and therapy. Nat Rev Cancer 2009; 9: 874-885.
[23] Turner J and Jones CE. Regulation of mucin expression in respiratory diseases. Biochem Soc Trans 2009; 37: 877-881.
[24] Woo HJ, Yoo WJ, Bae CH, Song SY, Kim YW, Park SY and Kim YD. Leptin up-regulates MUC5B expression in human airway epithelial cells via mitogen-activated protein kinase pathway. Exp Lung Res 2010; 36: 262-269.
[25] Iwakura Y, Ishigame H, Saijo S and Nakae S. Functional specialization of interleukin-17 family members. Immunity 2011; 34: 149-162.
[26] Nakajima T, Lin KW, Li J, McGee HS, Kwan JM, Perkins DL and Finn PW. T cells and lung injury. Impact of rapamycin. Am J Respir Cell Mol Biol 2014; 51: 294-299.
[27] Jones CE and Chan K. Interleukin-17 stimulates the expression of interleukin-8, growth-related oncogene-alpha, and granulocyte-colony-stimulating factor by human airway epithelial cells. Am J Respir Cell Mol Biol 2002; 26: 748-753.
[28] Kim D and Salzberg SL. TopHat-fusion: an algorithm for discovery of novel fusion transcripts. Genome Biol 2011; 12: R72.
[29] Kim D, Pertea G, Trapnell C, Pimentel H, Kelley R and Salzberg SL. TopHat2: accurate alignment of transcriptomes in the presence of insertions, deletions and gene fusions. Genome Biol 2013; 14: R36.
[30] DeLuca DS, Levin JZ, Sivachenko A, Fennell T, Nazaire MD, Williams C, Reich M, Winckler W and Getz G. RNA-SeQC: RNA-seq metrics for quality control and process optimization. Bioinformatics 2012; 28: 1530-1532.
[31] Trapnell C, Williams BA, Pertea G, Mortazavi A, Kwan G, van Baren MJ, Salzberg SL, Wold BJ and Pachter L. Transcript assembly and quantification by RNA-Seq reveals unannotated transcripts and isoform switching during cell differentiation. Nat Biotechnol 2010; 28: 511-515.
[32] Trapnell C, Hendrickson DG, Sauvageau M, Goff L, Rinn JL and Pachter L. Differential analysis of gene regulation at transcript resolution with RNA-seq. Nat Biotechnol 2013; 31: 46-53.
[33] Trapnell C, Roberts A, Goff L, Pertea G, Kim D, Kelley DR, Pimentel H, Salzberg SL, Rinn JL and Pachter L. Differential gene and transcript

expression analysis of RNA-seq experiments with TopHat and Cufflinks. Nat Protoc 2012; 7: 562-578.
[34] Florea L, Song L and Salzberg SL. Thousands of exon skipping events differentiate among splicing patterns in sixteen human tissues. F1000Res 2013; 2: 188.
[35] Roberts A, Pimentel H, Trapnell C and Pachter L. Identification of novel transcripts in annotated genomes using RNA-Seq. Bioinformatics 2011; 27: 2325-2329.
[36] Ge H, Liu K, Juan T, Fang F, Newman M and Hoeck W. FusionMap: detecting fusion genes from next-generation sequencing data at base-pair resolution. Bioinformatics 2011; 27: 1922-1928.
[37] van Haaften T, Byrne R, Bonnet S, Rochefort GY, Akabutu J, Bouchentouf M, Rey-Parra GJ, Galipeau J, Haromy A, Eaton F, Chen M, Hashimoto K, Abley D, Korbutt G, Archer SL and Thebaud B. Airway delivery of mesenchymal stem cells prevents arrested alveolar growth in neonatal lung injury in rats. Am J Respir Crit Care Med 2009; 180: 1131-1142.
[38] Inamdar AC and Inamdar AA. Mesenchymal stem cell therapy in lung disorders: pathogenesis of lung diseases and mechanism of action of mesenchymal stem cell. Exp Lung Res 2013; 39: 315-327.
[39] Blazquez R, Sanchez-Margallo FM, Alvarez V, Uson A and Casado JG. Surgical meshes coated with mesenchymal stem cells provide an anti-inflammatory environment by a M2 macrophage polarization. Acta Biomater 2016; 31: 221-230.
[40] Forman HJ, Aldrich TK, Posner MA and Fisher AB. Differential paraquat uptake and redox kinetics of rat granular pneumocytes and alveolar macrophages. J Pharmacol Exp Ther 1982; 221: 428-433.
[41] Hoet PH and Nemery B. Polyamines in the lung: polyamine uptake and polyamine-linked pathological or toxicological conditions. Am J Physiol Lung Cell Mol Physiol 2000; 278: L417-433.
[42] Jones AL, Elton R and Flanagan R. Multiple logistic regression analysis of plasma paraquat concentrations as a predictor of outcome in 375 cases of paraquat poisoning. QJM 1999; 92: 573-578.
[43] Sharp CW, Ottolenghi A and Posner HS. Correlation of paraquat toxicity with tissue concentrations and weight loss of the rat. Toxicol Appl Pharmacol 1972; 22: 241-251.
[44] Mitra S and Abraham E. Participation of superoxide in neutrophil activation and cytokine production. Biochim Biophys Acta 2006; 1762: 732-741.
[45] Bianchi M, Fantuzzi G, Bertini R, Perin L, Salmona M and Ghezzi P. The pneumotoxicant paraquat induces IL-8 mRNA in human mononuclear cells and pulmonary epithelial cells. Cytokine 1993; 5: 525-530.
[46] Tsantes A, Tsangaris I, Kopterides P, Kapsimali V, Antonakos G, Zerva A, Kalamara E, Bonovas S, Tsaknis G, Vrigou E, Maniatis N, Dima K and Armaganidis A. The role of procalcitonin and IL-6 in discriminating between septic and non-septic causes of ALI/ARDS: a prospective observational study. Clin Chem Lab Med 2013; 51: 1535-1542.
[47] Vargas-Rojas MI, Ramirez-Venegas A, Limon-Camacho L, Ochoa L, Hernandez-Zenteno R and Sansores RH. Increase of Th17 cells in peripheral blood of patients with chronic obstructive pulmonary disease. Respir Med 2011; 105: 1648-1654.
[48] Newcomb DC and Peebles RS Jr. Th17-mediated inflammation in asthma. Curr Opin Immunol 2013; 25: 755-760.
[49] Chang SH, Mirabolfathinejad SG, Katta H, Cumpian AM, Gong L, Caetano MS, Moghaddam SJ and Dong C. T helper 17 cells play a critical pathogenic role in lung cancer. Proc Natl Acad Sci U S A 2014; 111: 5664-5669.
[50] Kononova TE, Urazova OI, Novitskii VV, Churina EG, Kolobovnikova YV, Ignatov MV, Zakharova PA and Pechenova OV. Functional activity of Th-17 lymphocytes in pulmonary tuberculosis. Bull Exp Biol Med 2014; 156: 743-745.
[51] Rose MC and Voynow JA. Respiratory tract mucin genes and mucin glycoproteins in health and disease. Physiol Rev 2006; 86: 245-278.
[52] Hays SR and Fahy JV. Characterizing mucous cell remodeling in cystic fibrosis: relationship to neutrophils. Am J Respir Crit Care Med 2006; 174: 1018-1024.
[53] Groneberg DA, Eynott PR, Oates T, Lim S, Wu R, Carlstedt I, Nicholson AG and Chung KF. Expression of MUC5AC and MUC5B mucins in normal and cystic fibrosis lung. Respir Med 2002; 96: 81-86.
[54] Yuan-Chen Wu D, Wu R, Reddy SP, Lee YC and Chang MM. Distinctive epidermal growth factor receptor/extracellular regulated kinase-independent and -dependent signaling pathways in the induction of airway mucin 5B and mucin 5AC expression by phorbol 12-myristate 13-acetate. Am J Pathol 2007; 170: 20-32.
[55] Chen Y, Thai P, Zhao YH, Ho YS, DeSouza MM and Wu R. Stimulation of airway mucin gene expression by interleukin (IL)-17 through IL-6 paracrine/autocrine loop. J Biol Chem 2003; 278: 17036-17043.
[56] Hirai Y, Iyoda M, Shibata T, Kuno Y, Kawaguchi M, Hizawa N, Matsumoto K, Wada Y, Kokubu

F and Akizawa T. IL-17A stimulates granulocyte colony-stimulating factor production via ERK1/2 but not p38 or JNK in human renal proximal tubular epithelial cells. Am J Physiol Renal Physiol 2012; 302: F244-250.

[57] Inoue D, Numasaki M, Watanabe M, Kubo H, Sasaki T, Yasuda H, Yamaya M and Sasaki H. IL-17A promotes the growth of airway epithelial cells through ERK-dependent signaling pathway. Biochem Biophys Res Commun 2006; 347: 852-858.

[58] Hata K, Andoh A, Shimada M, Fujino S, Bamba S, Araki Y, Okuno T, Fujiyama Y and Bamba T. IL-17 stimulates inflammatory responses via NF-kappaB and MAP kinase pathways in human colonic myofibroblasts. Am J Physiol Gastrointest Liver Physiol 2002; 282: G1035-1044.

[59] Bulek K, Liu C, Swaidani S, Wang L, Page RC, Gulen MF, Herjan T, Abbadi A, Qian W, Sun D, Lauer M, Hascall V, Misra S, Chance MR, Aronica M, Hamilton T and Li X. The inducible kinase IKKi is required for IL-17-dependent signaling associated with neutrophilia and pulmonary inflammation. Nat Immunol 2011; 12: 844-852.

[60] Wang L, Tang L, Wang Y, Wang L, Liu X, Liu X, Chen Z and Liu L. Exendin-4 protects HUVECs from t-BHP-induced apoptosis via PI3K/Akt-Bcl-2-caspase-3 signaling. Endocr Res 2016; 41: 229-235.

[61] Yang T, Xu F, Sheng Y, Zhang W and Chen Y. A targeted proteomics approach to the quantitative analysis of ERK/Bcl-2-mediated anti-apoptosis and multi-drug resistance in breast cancer. Anal Bioanal Chem 2016; 408: 7491-7503.

[62] Zhang Q, Huang WD, Lv XY and Yang YM. Ghrelin protects H9c2 cells from hydrogen peroxide-induced apoptosis through NF-kappaB and mitochondria-mediated signaling. Eur J Pharmacol 2011; 654: 142-149.

[63] Seo HJ, Choi SJ and Lee JH. Paraquat induces apoptosis through cytochrome C release and ERK activation. Biomol Ther (Seoul) 2014; 22: 503-509.

[64] Yamada A, Aki T, Unuma K, Funakoshi T and Uemura K. Paraquat induces epithelial-mesenchymal transition-like cellular response resulting in fibrogenesis and the prevention of apoptosis in human pulmonary epithelial cells. PLoS One 2015; 10: e0120192.

Certificate of Analysis

Sprague-Dawley Rat Mesenchymal Stem Cells With GFP
Cryopreservation Date: 2016-07-25
Passage Number: 2

Catalog No. RASMX-01101
Lot Number: 160725R41

Viability

Cells are assayed for viability post-thaw using vital staining assay with trypan blue.
Specification: Cells should exhibit ≥ 80% viability.

Sterility

Bacterial and Fungal Contamination: Samples are inoculated and cultured on blood agar plate, thioglycolate broth, tryptocase soy broth and sabouraud dextrose agar.
Specification: No growth must be observed.

Mycoplasma: Samples are tested for mycoplasma contamination using a PCR-based assay and direct culture.
Specification: Results must be negative.

Endotoxin: Samples are tested for endotoxin contamination with LAL test.
Specification: Results must show a concentration of ≤ 25 EU/ml.

Purity

Cells are assayed for purity using flow cytometric analysis of cell surface antigen expression after cryopreservation. Cells are immunofluorescently stained with fluorochrome-conjugated antibodies specific to cell surface antigens CD90, CD34, CD44, CD45 and CD11b/c.
Specification: Cells must show ≥ 70% positivity for expression of cell surface antigens CD90 and CD44. Cells must show ≤ 5% positivity for expression of cell surface antigens CD34, CD45 and CD11b/c.

Proliferation ability

Cells are characterized by their ability to proliferate in culture with an attached well-spread morphology for ≥ 5 passages, and ≤ 5% cells exhibit spontaneous differentiation in each passage.

GFP expression

Expression of constitutive GFP is assayed by visual inspection of GFP fluorescence signal.
Specification: The results must indicate ≥80% of cells are visually inspected for GFP fluorescence signal during extensive subcultivation.

Differentiation ability

Cells are assayed after cryopreservation for their ability of tri-lineage differentiation. Cells must be able to differentiate to osteocytes, adipocytes and chondrocytes when cultured in the appropriate differentiation media.

Results

All specifications have been met.

Jane Chen
QA Manager
Aug 24, 2016